"Synchronized reinjection and coalescence of droplets in microfluidics"

Supplementary Information

Manhee Lee,[a,§] **Jesse W. Collins,**[b] **Donald M. Aubrecht,**[b] **Ralph A. Sperling,**[b,#] **Laura Solomon,**[c] **Jong-wook Ha,**[d] **Gi-Ra Yi,**[e] **David A. Weitz**[a,b]**, and Vinothan N. Manoharan**[*b,a]

[a] *Department of Physics, Harvard University, Cambridge, Massachusetts 02138, USA. Fax: +1 617 495 0416; Tel: +1 617 495 3763; E-mail: vnm@seas.harvard.edu*
[b] *School of Engineering and Applied Sciences, Harvard University, Cambridge, Massachusetts 02138, USA.*
[c] *College of Engineering, Temple University, Philadelphia, 19122, USA.*
[d] *Korea Research Institute of Chemical Technology, Daejeon 305-600, Korea.*
[e] *Department of Polymer Science and Engineering, Sungkyunkwan University, University, Suwon, 440-746 Korea.*
[§] *Current address: S. LSI, Giheung-campus, Samsung electronics, Yonginsi, 446-811, Korea.*
[#] *Current address: Institut für Mikrotechnik Mainz GmbH, Carl-Zeiss-Straße 18-20, 55129 Mainz, Germany.*

I. Synthesis of Fluorinated Surfactants

In the experiments, we synthesized and used two fluorinated surfactants [S1], surfactant I and surfactant II. Surfactant I was used in most experiments except the experiments using device III shown in Fig. 3(a,c). Here we describe the experimental protocol to synthesize surfactant I and II.

(1) Synthesis of Surfactant I

In a typical reaction, we dissolved 80 g of commercially available perflouro-polyether Krytox 157-FSH (DuPont, 12.3 mmol assuming 6500 g/mol) in an equal volume of HFE-7100 (3M) in a round flask and activated its terminal carboxylic group with a 10x molar excess of oxalyl chloride (10.4 mL, Sigma-Aldrich). The mixture became hazy and slightly yellow and was stirred overnight. Then, the solvent and unreacted oxalyl chloride were distilled off (70 °C and increased vacuum) and neutralized by bubbling the vapors through 2 M KOH. Then, the flask was attached to a rotation evaporator to remove all remaining traces of unreacted oxalyl chloride. The activated Krytox was allowed to cool down before diluting it in 50 mL HFE-7100, as all solvent had been evaporated in the previous process.

For the central hydrophilic block of the surfactant, a diamine PEG was used (Jeffamine ED900: O,O'-bis(aminopropyl) polypropylene glycol-b-polyethylene glycol-b-polypropylene glycol, x+z~6.0, y~12.5, a gift from Huntsman Chemicals), which yields one amino group with a few PPO units at each end. A stock solution was prepared by dissolving 6.6 g (14.8 mmol) in 100 ml anhydrous dichloromethane, and 50 ml HFE-7100 were added. The total amount of Jeffamine yields a 1.2x molar excess in regard the activated carboxylic groups from Krytox-158 FSH, assuming 6500 g/mol. Due to the presumably polydisperse reagents and the uncertainty of the number of molecules present, the stock solution was added stepwise to first favor the formation of triblock molecules with an excess of Krytox (assuming the nominal molecular weights), and then to saturate all remaining Krytox molecules. Both di- and triblock molecules, and even the plain Krytox with its carboxylic group, are surface-active molecules and effective in stabilizing the droplets.

Of the Jeffamine ED900 stock solution, 100 ml were added to the flask containing the activated Krytox to initiate the reaction, after 30 min another 25 ml were added, after another 30 min the remaining 25 ml. During the reaction, the flask was attached to the rotation evaporator, briefly heated after each addition, and then kept stirring at room temperature to avoid complete evaporation of the solvents. After rotating overnight, the temperature was set to 70 °C and vacuum was applied to evaporate all solvent. The final product was a milky-white viscous oil.

The material was diluted in ~50 ml HFE-7100 and collected into several 50 ml plastic centrifuge tubes (VWR, high g). A table spoon of plain PEG powder (100,000 g/mol, Sigma-Aldrich) was added to each tube and mixed with the samples by shaking. After centrifugation overnight, the sample separated into a clear bottom phase and a white top layer consisting of the excess of unreacted Jeffamine. The PEG powder helps to form a solid plug of upper phase that does not get redispersed too easily in the following processing step. With a sharp razor, we carefully cut into the bottom of the plastic tube and collected the clear fluorinated bottom fraction into a new tube. Residual material and turbid fractions were pooled and centrifuged again. After evaporation of the

solvent at 65°C over two days, the obtained material was viscous and clear, with a yellowish shade (Fig. S1.).

(2) Synthesis of Surfactant II

Perfluoropolyether (PFPE) block was first synthesized from the alkali metal fluoride catalyzed anionic oligomerization of hexafluoropropylene oxide (HFPO, 3M/Dyneon). In a 300 mL jacketed autoclave equipped with pressure gauge, thermocouple, inlet and outlet valves, 0.73 g of spray-dried solid potassium fluoride (KF, Sigma-Aldrich) and 15.0 g of tetraethylene glycol dimethyl ether (Sigma-Aldrich) were charged initially, and then the reactor was evacuated and filled with high purity nitrogen. Typically, three vacuum/nitrogen cycles were performed, and the pressure inside the reactor was adjusted to equilibrate with atmospheric condition with nitrogen. The suspension of KF was stirred for 1 hour at 25 °C. A cross-type magnetic spin bar was used to agitate the reaction media. 303.1 g of gaseous HFPO were introduced into the reactor during 6 hours. After finishing the addition of HFPO, the reaction mixture was stirred for sufficient time (typically for 2 hours) in order to consume almost all of the HFPO. The oligomerization product was transferred into a separation funnel, and the organic solvent layer was discarded after phase separation. The HFPO oligomer with acid fluoride end group was filtered and analyzed by gas chromatography (Younglin, M600D) in order to determine the molecular weight.
    The stabilizer consisting of fluorophilic-fluorophobic-fluorophilic blocks was synthesized as follows. 30 g (50 mmol) of O,O'-bis(aminopropyl) polypropylene glycol-b-polyethylene glycol-b-polypropylene glycol (Mn~600, Jeffamine ED600, x+z~3.6, y~9.0) was diluted in 90 g of Asahiklin AK-225 (Asahi Glass Company) solvent at room temperature. To this, a slight excess (100 g, 106 mmol) of PFPE (Mn~930, n~3.7) was slowly added with vigorous stirring. The formation of an amide linkage between amine and acid fluoride could be confirmed by FT-IR (Jasco FT/IR4000). After completion of the reaction, the crude product was washed in a NaHCO$_3$ aqueous solution twice and with deionized water until the pH of the aqueous phase was neutral. Finally, the PFPE-based stabilizer was recovered from solution by evaporating the solvent at reduced pressure. 107 g of yellowish viscous product were obtained (Fig. S1.).

Fig. S1. Chemical structure of the PFPE-PEG-PFPE surfactants: Surfactant I: n ~ 37, x + z ~ 6.0, y ~ 12.5. Surfactant II: n = 3.7, x + z ~ 3.6, y ~ 9.0.

    The molecular weight of the synthesized oligomers was also measured by chromatography (Fig. S2(a)). Gas chromatography (GC) analysis was performed with M600D GC system (Younglin Instrument, Korea) equipped with OV-1 capillary column (60 m × 0.25 mm ID × 0.25 μm, Ohio Valley Specialty Company, USA) and FID detector. The detector and injector temperatures were set at 280 °C. The oven temperature was programmed for 40 °C for 5 min, and reached 240 °C with a heating rate of 20 °C min^{-1} where it stayed for 20 min. In order to enhance the peak resolution, the acid fluoride end groups were transformed into methyl ester by reacting with methanol. After mixing the HFPO oligomer with a small portion of methanol in a vial, the by-product of HF and excess methanol were removed by washing with deionized water. The resulting PFPE methyl ester was treated by anhydrous magnesium sulfate and then filtered through a syringe filter before analysis. Finally, the PFPE methyl ester was diluted with 1,1,2-trichlorotrifluoroethane (Freon-113). Because the GC analysis provides the weight-averaged molecular weight, it is possible to estimate the polydispersity index (M_w/M_n) of PFPEs from the following relationships: $M_n = \sum_i n_i M_i / \sum_i n_i$ and $M_w = \sum_i n_i M_i^2 / \sum_i n_i M_i$, where n_i represents the GC area percent and M_i is molar mass of the i-mer. The synthesized PFPE showed M_n~940 and M_w ~960.
    The FT-IR spectrum of PFPE (Fig. S2(b)) showed two characteristic peaks denoting two different end groups: acid fluoride (COF, 1885 cm^{-1}) and carboxylic acid (COOH, 1778 cm^{-1}), but this might have resulted from rapid reaction of acid fluoride with atmospheric moisture during the sample preparation and analysis. Neat Jeffamine ED 600 shows NH bending and stretching vibrations at 1594 cm^{-1} and 3350 cm^{-1}. In the IR spectrum of the

synthesized stabilizer, new peaks appear at 1716 cm^{-1} and 1548 cm^{-1}, representing C=O stretching of the carbonyl group and amide II band. CH$_2$ stretching and scissoring bands at 2860 and 1450 cm^{-1} originate from Jeffamine. There is no indication of unreacted PFPE.
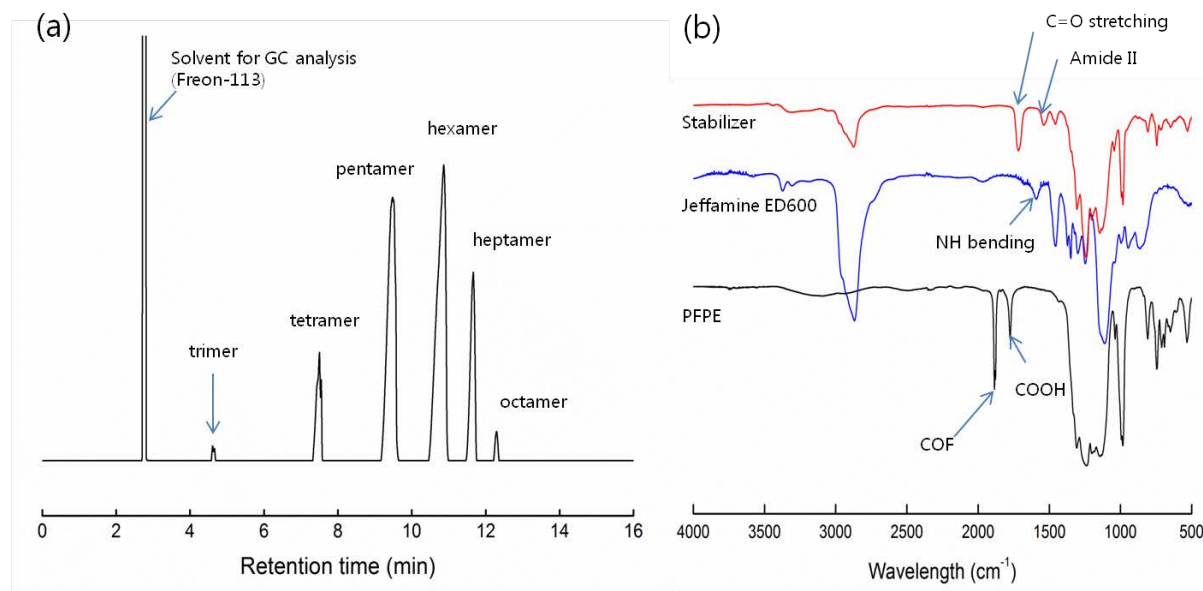

Fig. S2. (a) Gas Chromatography of PFPE (HFPO oligomer). (b) FT-IR analysis of PFPE surfactant.

II. Measurement of Oil-Water Interfacial Tension

Interfacial tensions play a key role in the formation, reinjection, and coalescence of droplets in our experiments. In particular, the coalescer in our study requires holding one droplet at the coalescence junction until the other droplet comes and touches it. The droplet is held at the junction under the condition, $Q_b R_b < P_{ra}^{c} \sim 2\gamma/l_a$, as described in the manuscript. Here we present the simple microfluidic method we used to measure the interfacial tension between oil and water by using hydrostatic pressure in conjunction with a conventional syringe pump.

Figure S3(a) shows the microfluidic tensiometer, operated by two hydrostatic pressures P_i and P_o and one syringe pump. We inject the oil (HFE-7500) containing the desired surfactant into the device at a constant flow rate Q_m using a syringe pump while applying hydrostatic pressures P_i to upper chamber filled with the aqueous phase (DI-water) and P_o to the outlet of the device. By modelling the fluidic system with an equivalent circuit, we obtain a simple relation between P_{io} (=P_i-P_o) and the curvature of the aqueous phase r_L (red arrow in Fig. S3(a).),

$$P_{io} = \gamma \left(\frac{1}{r_L} + \frac{1}{h} \right) + R_m Q_m , \qquad (S1)$$

where γ is the interfacial tension, h the height of the channel, and R_m the fluidic resistance of the main channel indicated in Fig. S3(a). For a given Q_m, r_L varies depending on P_{io}. Once we get a curve of P_{io} as a function of $1/r_L$, γ is then simply given by the slope of the curve. Figure S3(b) shows the experimentally measured P_{io} and $1/r_L$ when using the oil (HFE-7500) and surfactant I. We get γ=3.7x10^{-3} N/m from the slope of the linear fit (black curve in Fig. 2(b)). We also used the traditional pendant-drop method to measure γ. Since the density of water (1.0 g/ml) is very different from that of the oil (1.6 g/ml), water drops were often ruptured during the operation, preventing an accurate measurement. Still, we find an interfacial tension on the order of 5x10^{-3} N/m.
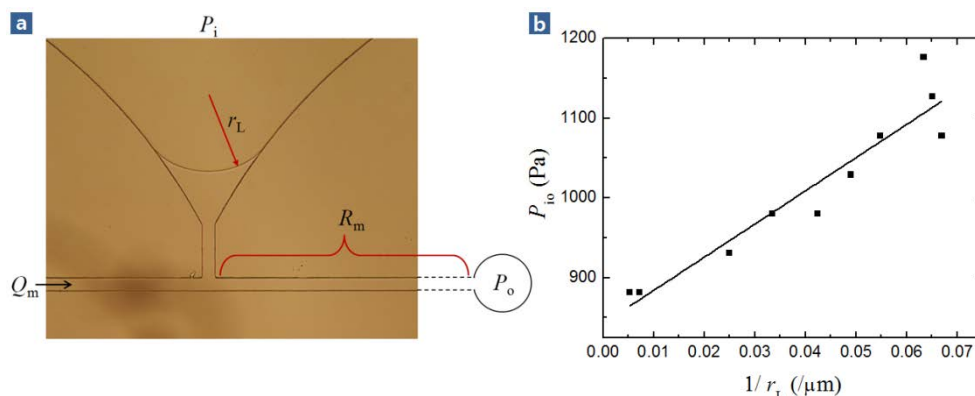
Fig. S3. Measurement of interfacial tension using microfluidic tensiometer. (a) Optical micrograph of our microfluidic tensiometer, which consists of a constant flow of surfactant-dissolved oil driven by a syringe pump, with the aqueous phase in the upper chamber subject to hydrostatic pressure P_i, and the outlet to pressure P_o. (b) Experimentally measured P_{io} (=P_i - P_o) as a function of $1/r_L$ and linear fit using Eq. (S1)

III. Yield Analysis

The final yield of reinjection and coalescence of droplets depends on the initial orderings of droplets reinjected. Let us represent the array of droplets as an ordered set S={$a(1)$, $a(2)$,…,$a(N)$}, where N is the total number of droplets injected and $a(i)$ is defined as 1 if a droplet came out from the upper chamber or 0 if otherwise. Then, the number of wrong coalescences (W), coalescence of droplets from same chamber, is given as $W = \sum_{i=1}^{N/2} \delta_{a(2i-1),a(2i)}$ where δ_{ij} is the Kronecker Delta. The number of order changes (NOC) of reinjection defined in the manuscript is represented as $\text{NOC} = \sum_{i=1}^{N} \delta_{a(i),a(i+1)}$, which can be rearranged as $\text{NOC} = \sum_{i=1}^{N/2} \delta_{a(2i-1),a(2i)} + \sum_{i=1}^{N/2} \delta_{a(2i),a(2i+1)}$. If we assume translation symmetry in the droplet array, the second part becomes the same as the first part of the rearranged NOC (by 2i→2i+1), and thus E=NOC/N=2W/N. From the definition of yield (Y), Y≡(N/2–W)/(N/2), we finally get Y=1-E.

IV. Synchronized Reinjection of Droplets and Their Size Distributions

There are many factors that affect the synchronized reinjection in our devices, including the size distribution of droplets, the externally applied hydrostatic pressures, and material properties such as the interfacial tension and viscosity in the upper and lower chambers (Fig. 3(a) in the manuscript). For the size-distribution, it is obvious that if the sizes of the two droplets that meet at the junction are very different, then the injection of droplets does not alternate. One may therefore expect that the synchronized reinjection of droplets becomes worse as the mean diameters of the droplets in the two chambers differ more. In this section, we present a preliminary data supporting this conjecture.

Figure S4 shows a set of three experiments using device I with emulsions I, II and III. Each emulsion consists of two kinds of droplets; droplets made with DI-water in the upper chamber and droplets made with DI-water containing dye (Allura Red, SigmaAldrich) in the lower chamber. They were prepared in the same way using flow-focusing and were reinjected into device I. Through image analysis of optical micrographs, we investigated the diameter distributions of close-packed droplets in the upper and lower chambers of the device before they were released into the main flow channels. We find that the error rate increases as the difference in the mean diameters of the droplets in the upper (red bars) and lower (black bars) chambers increases, even when balancing the pressure P_u and P_l, (Fig. 3(a) in the manuscript) as well as possible (Fig. S4 and Table S1).
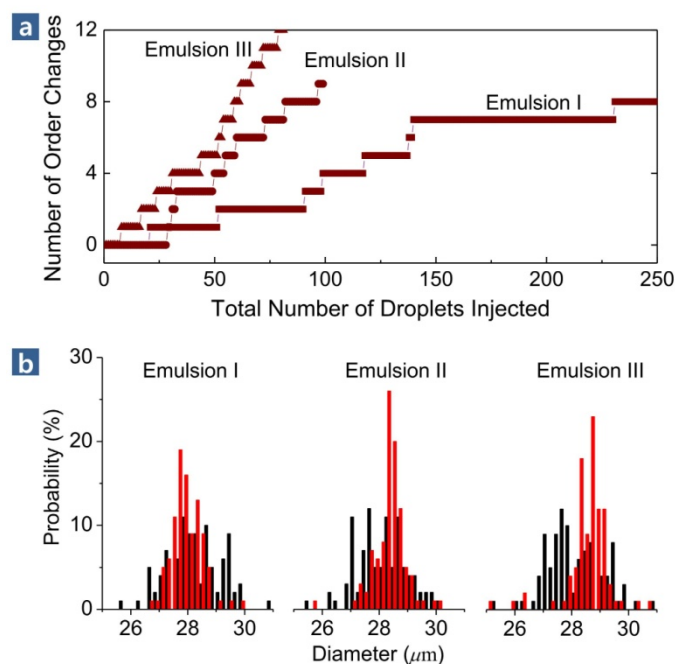
Fig. S4. Error rates in reinjecting droplets and their diameter distributions. (a) Number of order changes as a function of total number of droplets injected for emulsions I, II, and III using device I. (b) Diameter distributions of droplets in upper (red bars) and lower (black bars) chambers. We selected 100 droplets in each chamber and determined the diameter by taking optical micrographs and counting the number of pixels in each droplet.

	Emulsion I		Emulsion II		Emulsion III	
	Upper Chamber	Lower Chamber	Upper Chamber	Lower Chamber	Upper Chamber	Lower Chamber
Mean Diameter (μm)	27.9	28.3	28.3	27.8	28.8	28.0
Standard Deviation (μm)	1.0	1.3	0.9	1.5	1.7	1.2

Table S1. Statistics of droplet diameters for emulsions I, II and III in Fig. S4(b).

V. Trap and Coalescence of Multiple Droplets (See also ESI 4)

In the manuscript, we demonstrated a coalecer that traps one droplet and fuses the trapped droplet with another droplet. For a given droplet volume (V) and flow rate of the carrier oil (Q_m) we achieved coalescence by regulating the drain pressure P_{do}. In this section, we show that this scheme works also for trapping and coalescencing multiple droplets, which was also realized experimentally as shown in ESI 4.

Let us first consider Eq. (2) in the manuscript, where $R_b(V)$ is an increasing function of the droplet volume V. By replacing V by $2V$ and $3V$, we can plot two other curves from Eq. (2) with $R_b(2V)$, and similarly Eq. (2) with $R_b(3V)$, which have lower intercept points (see Eq. (2) of the manuscript). Such curves can be found experimentally, but in the cartoon shown in Fig. S4 we present two hypothetical curves for explanatory purposes. The plot shows that one can easily find a specific regime in which a specific number of droplets become trapped.

For example, when operating under a condition $Q_m=Q$ and $P_{do}=P$ (black circle in Fig. S5), a droplet with volume V that comes into the coalescer is trapped, because the condition satisfies the trap condition, $P_{do} < P^c_{do}(V)$ (black curve in Fig. S5; see manuscript for details). When the next droplet comes in, the two droplets are coalesced into a single droplet with volume $2V$ under an electric-field. From the diagram, we find that the big

droplet with volume $2V$ cannot be trapped and therefore exits the coalescer, because $P_{do} > P^c_{do}(2V)$. Now let us decrease the drain pressure to $P_{do}=P'$ at the fixed $Q_m=Q$. The new operating condition, marked as a blue circle in Fig. S5, lies in $P^c_{do}(3V) < P_{do} < P^c_{do}(2V)$, and therefore the regime results in two droplets being trapped and three droplets coalescenced. The trapping and coalescence of a controlled number of droplets by varying P_{do} is demonstrated in ESI 4 experimentally and can in principle be extended to coalesce more than three droplets.
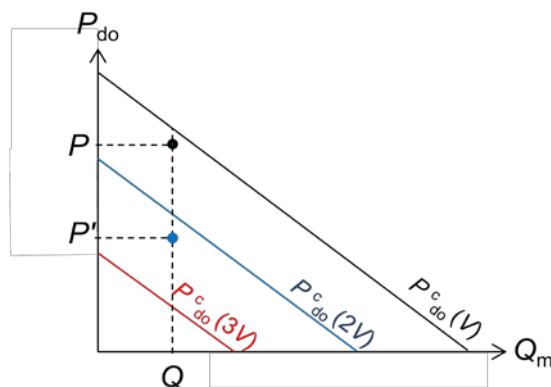

Fig. S5. State diagram of trap and coalescence of multiple droplets for the coalescer shown in Fig. 4(c) of the manuscript. The black curve represents Eq. (2) with $R_b(V)$ (as shown in the manuscript), the blue curve a hypothetical curve of Eq. (2) with $R_b(2V)$, and the red another hypothetical curve with $R_b(3V)$. The operating condition (P, Q) marked as black circle lies between $P^c_{do}(2V) < P_{do} < P^c_{do}(V)$, which results in one droplet being trapped and two droplets coalescencing. Then, by decreasing P_{do} to $P_{do} = P'$ (blue circle), one can make the operating condition lie in $P^c_{do}(3V) < P_{do} < P^c_{do}(2V)$, which results in two droplets being trapped and three droplets coalescencing. The trapping and coalescence of a controlled number of droplets is demonstrated in ESI 4 experimentally.

Reference

[S1] C. Holtze *et al.*, "Biocompatible Surfactants for Water-in-fluorocarbon Emulsions." *Lab on a Chip*, 2008, **8**, 1632–1639.